Available online at www.sciencedirect.com

SciVerse ScienceDirect

Ceramics International 38 (2012) 5827–5833

CERAMICS INTERNATIONAL

www.elsevier.com/locate/ceramint

Microstructure of new composite electrocatalyst and its anodic behavior for chlorine and oxygen evolution

M. Spasojević [a,*], L. Ribić-Zelenović [a], P. Spasojević [b]

[a] Joint Laboratory for Advanced Materials of the Serbian Academy of Science and Arts, Section for Amorphous Systems, Faculty of Agronomy Čačak, University of Kragujevac, Serbia

[b] Faculty of Technology and Metallurgy, University of Belgrade, Karnegijeva 4, 11000 Belgrade, Serbia

Received 28 March 2012; received in revised form 10 April 2012; accepted 10 April 2012
Available online 16 April 2012

Abstract

The first layer of active coating made from a rutile-structured solid solution of ruthenium and titanium dioxides having an average crystal grain size of 30 nm was thermally deposited on an adequately prepared titanium metal substrate. Then, at a temperature of 500 °C, the second layer was formed on the first layer from a mixture of amorphous particles of metallic platinum and rutile-structured iridium dioxide nanocrystals having an average crystal grain size of 26 nm.

Rutile phase nanocrystals are characterized by a high density of chaotically distributed dislocations and high internal microstrain values. The coatings exhibit a compact granular morphology without cracks on the surface. Their catalytic activity is similar to that of conventional DSAs for the anodic oxidation of chloride ions from both concentrated and dilute sodium chloride solutions. The anodic current efficiency both during chlorate formation and active chlorine production was several percentage points higher in electrolyzers containing these anodes than in those containing DSAs. The catalytic activity of anodes having these coatings is about 50 mV lower than that of DSAs and about 350 mV higher than that of lead/antimony alloy electrodes, for oxygen evolution from acid sulfate solutions (0.5 mol dm^{-3} H_2SO_4) characteristic of processes for the production of some metals. An accelerated corrosion test showed that the stability of the double-layer anodes is about twelve-fold higher than that of conventional DSAs.

Keywords: B. X-ray methods; B. Porosity; C. Corrosion; E. Electrodes

1. Introduction

Dimensionally stable anodes (DSA) have a wide use in the electrochemical industry, i.e. in chlor-alkaline and chlorate electrolysis as well as in cells for active chlorine production [1–37]. These processes generally use conventional DSAs composed of a titanium metal substrate coated with a thin active layer of rutile-structured 40 mol.%RuO_2 and 60 mol.%TiO_2 nanocrystalline solid solution by thermal deposition [1–37]. Conventional DSAs also have a high catalytic activity for oxygen evolution from acid sulfate solutions. However, their active layer relatively rapidly dissolves in these solutions. A poorly conductive titanium oxide layer is simultaneously formed in the titanium metal–coating interphase [38–41]. Therefore, these electrodes cannot be used in electroplating and metal electrowinning or in proton exchange membrane water electrolysis.

DSAs coated with an active layer of iridium dioxide or a nanocrystalline mixture of iridium dioxide and metallic platinum have a higher corrosion stability as compared to conventional DSAs in electrolytic chlorine, chlorate and active chlorine production. Moreover, with the use of these anodes, chlorine, chlorate and active chlorine are obtained at higher anodic current efficiencies [42–47]. However, the price of these anodes is higher due to a higher price of iridium and platinum salts than that of ruthenium salts.

Recently, research into the development of active coatings showing a high corrosion stability and high catalytic activity for oxygen evolution from acid sulfate solutions has been intensified for their use in electroplating and metal electrowinning as well as in proton exchange membrane water

* Corresponding author at: Faculty of Agronomy Čačak, University of Kragujevac, Cara Dušana 34, 32000 Čačak, Serbia. Tel.: +381 32 303402; fax: +381 32 303402.
E-mail address: ljiljana.spasojevic51@yahoo.com (M. Spasojević).

0272-8842/$36.00
http://dx.doi.org/10.1016/j.ceramint.2012.04.032

electrolysis [48–60]. These studies mostly focus on coatings containing nanocrystals of metallic platinum, iridium and ruthenium dioxides, and oxides of some non-precious metals (SnO_2, Sb_2O_5, and Ta_2O_5) [48–60].

The objective of this study was to develop novel active coatings made from metallic platinum and ruthenium, iridium and titanium oxides, and examine their microstructure and electrochemical behavior in chloride and acid sulfate solutions.

2. Experimental

A 10 g m^{-2} active film of a 40 mol.%RuO_2, 60 mol.%TiO_2 solid solution was thermally deposited on an adequately prepared titanium metal substrate [12–14]. A 2% solution of H_2PtCl_6 and $IrCl_3$ (referring to plain metals) in 2-propanol was deposited onto the first layer. The Pt to Ir ratio was 60–40. After deposition of the solution, the electrode was dried at 50 °C until complete evaporation of the solvent. Upon solvent evaporation, the electrode was heated for 10 min at 450 °C. The solution deposition process and the thermal treatment of the electrode were repeated until a 6 g m^{-2} coating (referring to plain metals) was made. Following the last deposition of the solution, the electrode was thermally treated for 60 min at 500 °C. The coating obtained is dark gray. An X-ray analysis was employed to examine its crystalline structure using a Philips diffractometer equipped with a graphite monochromator and Cu Kα radiation. The morphology of the coatings was examined using scanning electron microscopy, SEM (JEOL.JSM 5300 equipped with an EDS-QX2000 spectrometer).

Electrochemical measurements were performed in a standard 1.0 dm^3 glass electrochemical cell containing a saturated calomel electrode which was used as the reference electrode and placed in a separate compartment. A 4 cm^2 plate and a 25 cm^2 titanium metal plate served as the working electrode and the counter electrode, respectively. A standard electrical circuit composed of a programmer equipped with a potentiostat (RDE3 POTENTIOSTAT Pine Instrument Co., Grove City, PA), an X-Y recorder (Hewlett Packard 7035 B) and a digital voltmeter (Pro's Kit 03-9303C) was used in the experiment. The solutions were prepared from triple-distilled water and Merck chemicals. The anodic current efficiency for chlorate and active chlorine production was determined based on the composition of gaseous mixtures created in electrolytic cells [7]. Potentiometric titration with sodium arsenate(III) was used to determine the content of active chlorine in the solution [7].

3. Results and discussion

Upon deposition of the first layer, X-ray diffraction analysis was made for its phase structure (Fig. 1).

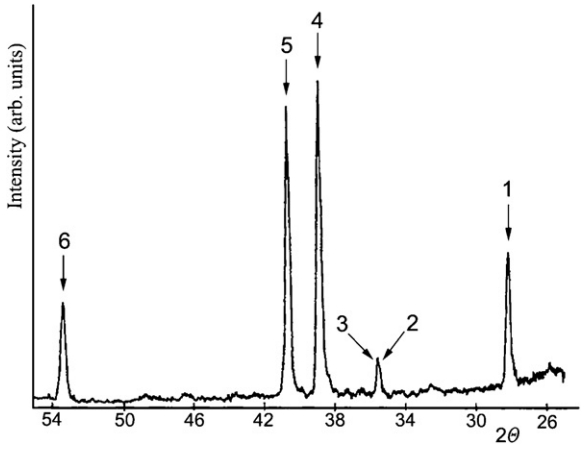

Fig. 1. X-ray diffraction pattern for the 40 mol.%RuO_2, 60 mol.%TiO_2 composite electrocatalyst.

The X-ray diffraction pattern shows peaks for the rutile-structured solid solution of RuO_2 and TiO_2 as well as peaks for different crystalline planes of the titanium metal substrate (Fig. 1 and Table 1).

No peaks for pure RuO_2 and pure TiO_2 are observed in the X-ray diffraction pattern. This suggests that these dioxides do not form separate phases and that their total amounts are present in the solid solution having a rutile crystal structure. The average crystal size is 30 nm. The rutile phase is characterized by a relatively high density of chaotically distributed dislocations and high internal microstrain values.

EDX spectra show that the coatings also contain small amounts of chlorine, as confirmed in previous studies [1,5,55]. The residual chlorine increases internal microstrains, causing dislocations. Chlorine atoms most likely replace oxygen atoms in the crystal lattice, thereby ensuring the formation of Ru^{3+} ions.

Upon thermal deposition of the second layer, X-ray analysis was used to determine the phase structure of the double-layer coating. Apart from the peaks for the titanium metal substrate and those for the solid solution of RuO_2 and TiO_2, the X-ray diffraction pattern shows the existence of peaks for the rutile phase of IrO_2 (Fig. 2, Table 2).

The lattice parameters of IrO_2 are slightly distorted from those for pure IrO_2 by about 0.2%. This may be the result of the inclusion of small quantities of residual chlorine or due to other irregularities in the normal lattice arrangement associated with non-stoichiometric composition. Residual chlorine atoms in the crystal lattice probably serve as a replacement for oxygen atoms thereby ensuring the emergence of Ir^{3+} ions. The resulting Ir^{3+} ions serve as active centers for some electrochemical reactions. The rutile phase of IrO_2 is characterized by a high density of chaotically distributed dislocations and high

Table 1
Peak structure.

Peak number	1	2	3	4	5	6
Structure	$RuO_2 + TiO_2$ (1 1 0)	$RuO_2 + TiO_2$ (1 0 1)	Ti (1 0 0)	Ti (0 0 2)	Ti (1 0 1) and $RuO_2 + TiO_2$ (1 1 1) and (2 0 0)	Ti (1 0 2)

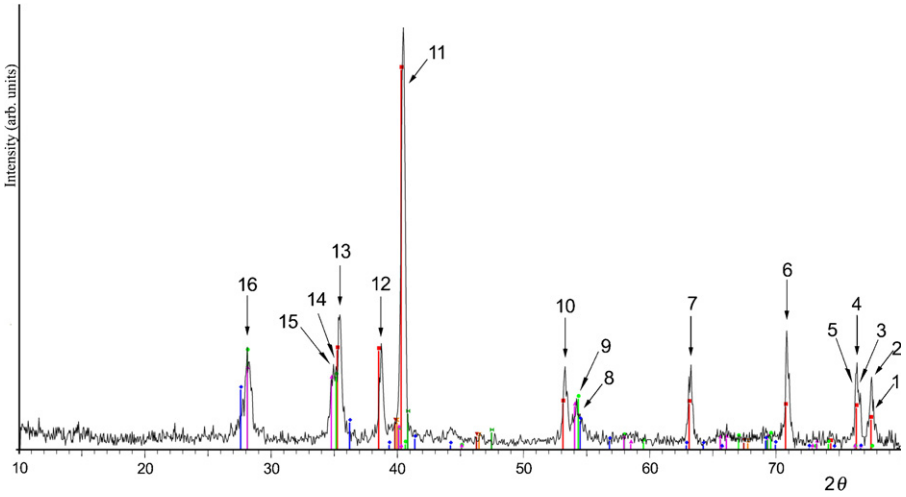

Fig. 2. X-ray diffraction pattern for the composite electrocatalyst containing RuO_2, TiO_2, IrO_2, Pt.

Table 2
Peak structure.

Peak no.	1	2	3	4	5	6	7
Structure	Ti (2 0 1)	$RuO_2 + TiO_2$ (2 1 2)	IrO_2 (2 1 2)	Ti (1 1 2)	$RuO_2 + TiO_2$ (3 2 0), IrO_2 (3 2 0)	Ti (1 0 3)	Ti (1 1 0)

8	9	10	11	12	13	14	15	16
$RuO_2 + TiO_2$(2 1 1)	IrO_2 (2 1 1)	Ti (1 0 2)	Ti (1 0 1), $RuO_2 + TiO_2$(1 1 1) IrO_2 (1 1 1), $RuO_2 + TiO_2$(2 0 0) IrO_2 (2 0 0)	Ti (0 0 2)	Ti (1 0 0)	$RuO_2 + TiO_2$ (1 0 1)	IrO_2 (1 0 1)	$RuO_2 + TiO_2$ (1 1 0), IrO_2 (1 1 0)

internal microstrains. The average crystal size of this phase is 26 nm.

The X-ray pattern presented in Fig. 2 does not show pronounced peaks for metallic platinum and its oxides. Comninellis and Vercesi [61,62] report that the thermal decomposition of H_2PtCl_6 results in PtO_x with x less than 0.2, i.e. a composition close to metallic Pt. This suggests that the platinum in the coating mostly occurs in the metallic state, exhibits an amorphous structure and has cluster-shaped particles most likely distributed in the IrO_2 rutile phase matrix. EDX spectra show that the atomic ratio of platinum to iridium in the coating is almost identical to that in H_2PCl_6 and $IrCl_3$ solution.

The morphology of the coatings is affected by the method of their formation. The coatings formed at 500 °C exhibit granular morphology with no cracks on the surface. The coatings formed at temperatures higher than 550 °C develop cracks. An increase in temperature results in an abrupt increase in both the number of cracks and crack width. The accelerated cooling of electrodes after the thermal treatment induces the development of a large number of wide cracks [5,6,63]. The cracks on the anode surface enhance anode degradation. Both the electrolyte and the anodically evolved oxygen penetrate the crack and reach the titanium metal substrate, oxidizing it and forming poorly conductive titanium oxides. The oxides that develop in the titanium metal–coating interphase cause anode passivation [5,6,38–41,64–69].

The real surface area of conventional DSAs is substantially larger than the geometric surface area [1,2,5–7,55,58,68,69]. Their real surface area comprises a rough outer surface area and an inner surface area composed of a micropore-containing surface area and a crack-like surface area [21,68]. The real surface areas of double-layer coatings were estimated using voltammetric charges obtained by current integration over time within the potential range of 0.25 V to 1.25 V from cyclic voltammograms obtained for the 0.5 mol dm^{-3} H_2SO_4 solution. Fig. 3. presents the cyclic voltammogram of the RuO_2, TiO_2, IrO_2, Pt anode.

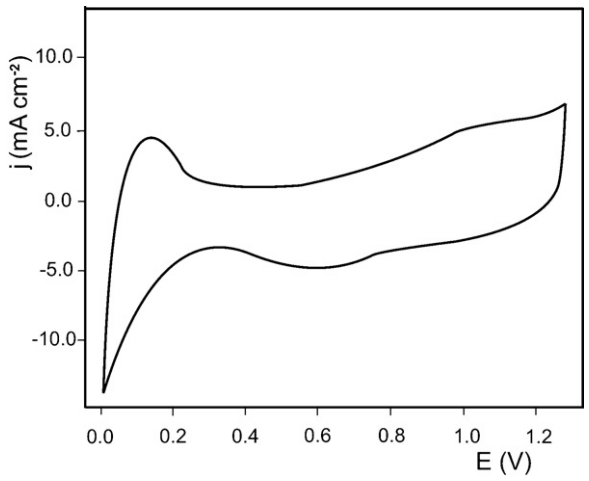

Fig. 3. Cyclic voltammograms of the RuO_2, TiO_2, IrO_2, Pt electrode in 0.5 H_2SO_4 at 25 °C. Potential sweep rate 100 mV s^{-1}.

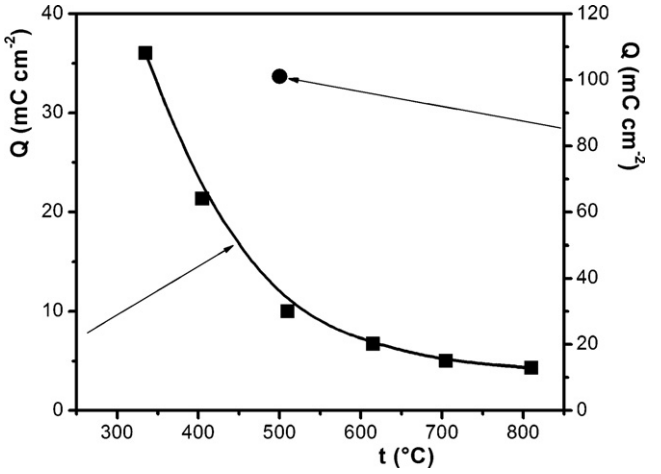

Fig. 4. Integrated voltammetric charges for: ■ – RuO_2, TiO_2, IrO_2, Pt electrodes as a function of the thermal treatment temperature; ● – IrO_2 electrode.

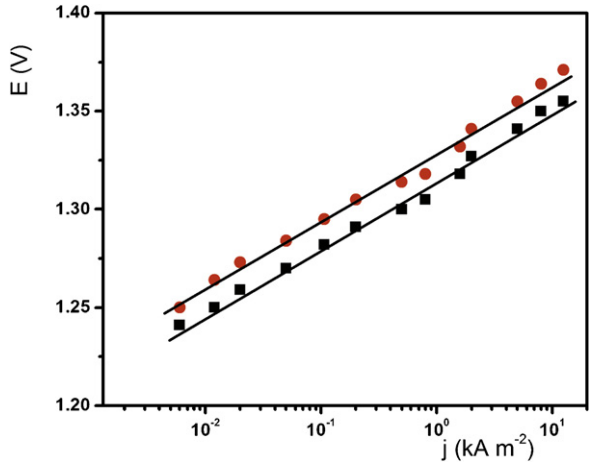

Fig. 5. Polarization characteristics of catalytic coatings of titanium anodes for chlorine evolution reaction: ■ – 40 mol.%RuO_2, 60 mol.%TiO_2; ● – RuO_2, TiO_2, IrO_2, Pt (300 g dm^{-3} NaCl, pH 2, t = 80 °C).

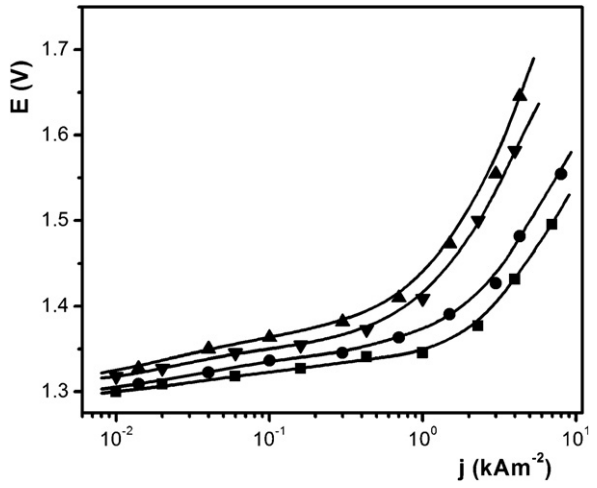

Fig. 6. Polarization characteristics of catalytic coatings of titanium anodes for the anodic oxidation of chloride ions: ■ – 40 mol.%RuO_2, 60 mol.%TiO_2; ● – RuO_2, TiO_2, IrO_2, Pt; (30 g dm^{-3} NaCl, pH 7, t = 25 °C). ▼ – 40 mol.%RuO_2, 60 mol.%TiO_2; ▲ – RuO_2, TiO_2, IrO_2, Pt (20 g dm^{-3} NaCl, pH 7, t = 25 °C).

The shape of the cyclic voltammogram is similar to that for polycrystalline platinum. This implies that the surface of the active double-layer coating is enriched with platinum atoms. Based on both the size of the peak for the desorption of adsorbed hydrogen atoms and the position of the potential of the maximum oxide reduction peak, the double-layer coating surface was roughly estimated to contain about 65 at.% of platinum atoms.

Fig. 4. presents the voltammetric charge as a function of temperature for active double-layer RuO_2, TiO_2, IrO_2, Pt coating formation. For illustration purposes, the same figure shows the charge value for the IrO_2 coating formed at 500 °C.

Fig. 4 shows that the voltammetric charge of the RuO_2, TiO_2, IrO_2, Pt anode is approximately eleven times lower than that of the IrO_2 electrode formed at the same temperature. RuO_2 coatings and coatings of a solid solution of RuO_2 and IrO_2 also have a considerably higher voltammetric charge as compared to the double-layer RuO_2, TiO_2, IrO_2, Pt coating. Da Silva et al. [55] and Yi et al. [31] found that increasing platinum content in the platinum and iridium dioxide coating induces a decrease in its voltammetric charge, suggesting that the platinum present hampers crack formation and micropore development, thereby leading to the formation of relatively more compact coatings. The thermal process of coating formation at 500 °C probably results in the formation of platinum clusters that position themselves around IrO_2 crystal grains. These clusters prevent crack development around IrO_2 crystal grains, hold back their further growth, cause the formation of a large number of chaotically distributed dislocations and induce increased internal microstrains in the grains. The good contact and the large contact area between amorphous platinum clusters and iridium dioxide nanocrystals likely contribute to the effect of the exchange integral i.e. energy of exchange between platinum nuclei and iridium nuclei on the electronic state of their atoms. All of the effects analyzed determine, in a particular way, the electrochemical behavior of RuO_2, TiO_2, IrO_2, Pt coatings.

Fig. 4. shows an abrupt decrease in the amount of anodic charge with increasing temperature within the temperature range of 300–500 °C, as opposed to the very slow decrease in the 600–800 °C interval. At higher temperatures, the sintering effect is more pronounced; hence the reduction in both the real surface area and the anodic charge.

The catalytic activity of the novel double-layer RuO_2, TiO_2, IrO_2, Pt electrode was examined for the reaction of anodic oxidation of chloride ions both from concentrated (Fig. 5) and dilute solutions (Fig. 6).

The diagrams in Figs. 5 and 6 show that the double-layer RuO_2, TiO_2, IrO_2, Pt coating has a high catalytic activity, similar to that of a conventional DSA, for the anodic oxidation of chloride ions from concentrated and dilute solutions of alkaline chlorides.

The anodic current efficiency during electrolytic chlorate production in cells using RuO_2, TiO_2, IrO_2, Pt anodes is several percentage points higher than in cells using conventional DSAs. The gaseous mixture exiting the chlorate cell containing RuO_2, TiO_2, IrO_2, Pt anodes during the electrolysis of 200 g dm^{-3}

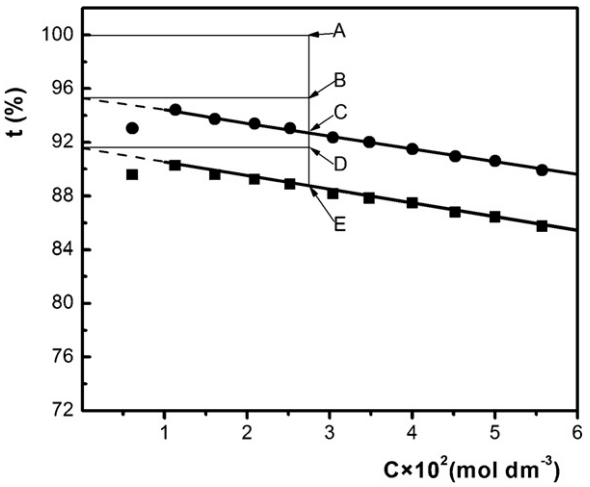

Fig. 7. Anodic current efficiency as a function of hypochlorite concentration: ■ – 40 mol.%RuO_2, 60 mol.%TiO_2; ● – RuO_2, TiO_2, IrO_2, Pt (30 g dm^{-3} NaCl, pH 7.5, t = 25 °C, j = 1.0 kA m^{-2}).

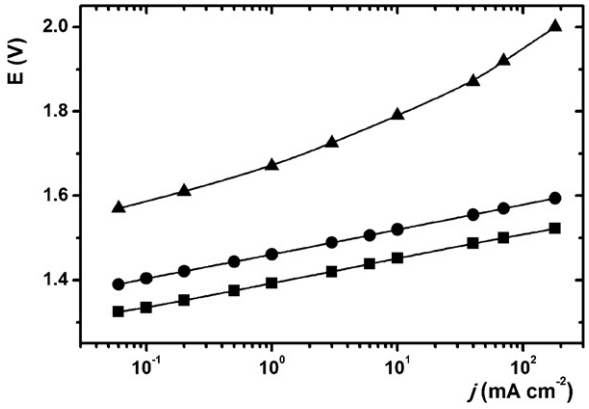

Fig. 8. Polarization characteristics for oxygen evolution for: ▲ – Pb (Sb); ■ – 40 mol.%RuO_2, 60 mol.%TiO_2; ● – RuO_2, TiO_2, IrO_2, Pt (0.5 mol dm^{-3} H_2SO_4, 0.6 mol dm^{-3} $CuSO_4$, t = 25 °C).

NaCl, 500 g dm^{-3} $NaClO_3$ and 3 g dm^{-3} $Na_2Cr_2O_7$ solution at t = 85 °C and pH 6.7 and at j = 3.0 kA m^{-2} contains 1.3–1.5% oxygen, whereas the gas exiting the DSA cells contains 2.4–3.0% oxygen.

The anodic current efficiency for active chlorine formation by the electrolysis of dilute solutions of sodium chloride is about 4% higher in electrolyzers containing RuO_2, TiO_2, IrO_2, Pt than in those containing DSA (Fig. 7).

Anodic current losses during chlorate formation and active chlorine production are attributed to the diffusionally controlled anodic oxidation of active chlorine (BC and DE) (Fig. 7) and activation-controlled anodic oxidation of water (AB and AD) (Fig. 7) [7]. Cells containing RuO_2, TiO_2, IrO_2, Pt anodes have a higher anodic current efficiency due to the higher activation overpotential of the anodic oxidation of water at these electrodes as compared to the overpotential at DSAs (Fig. 7).

The potential use of RuO_2, TiO_2, IrO_2, Pt anodes in the production of some metals (Cu, Zn, etc.) from their dilute acid sulfate solutions was examined. The catalytic activity was determined by recording polarization curves for oxygen evolution from the solution 0.5 mol dm^{-3} H_2SO_4, 0.6 mol dm^{-3} $CuSO_4$ (Fig. 8).

For comparison purposes, Fig. 8 shows polarization curves not only for RuO_2, TiO_2, IrO_2, Pt anodes but also for DSA and conventional industrial lead/antimony alloy electrodes (Pb(Sb)). Fig. 8 shows that, within the current density range characteristic of the production of some metals (Cu, Zn, etc.) from their dilute acid sulfate solutions, the catalytic activity of DSA is about 50 mV higher than that of RuO_2, TiO_2, IrO_2, Pt anodes. However, conventional Pb(Sb) anodes have about 350 mV lower catalytic activity. During electrolysis, Pb(Sb) anodes corrode and contaminate the solution, due to which metals containing small amounts of lead, rather than plain metals, are obtained on the cathode.

The stability of a conventional DSA, a titanium anode containing a 60 mol.%Pt, 40 mol.%IrO_2 coating and a novel double-layer RuO_2, TiO_2, IrO_2, Pt electrode was estimated using the accelerated corrosion test. The test involved monitoring of the dependence of the change of the anode potential on the time of electrolysis of 0.5 mol dm^{-3} H_2SO_4 solution at 25 °C and at current density of 1000 mA cm^{-2}. During the initial interval of time, the potential gradually increases. After a while, there is a sudden increase in the potential. The size of the initial interval of time denotes the anode stability time. The rapid corrosion test shows that the stability of RuO_2, TiO_2, IrO_2, Pt anodes is about twelve times that of conventional DSAs and about two times that of titanium anodes coated with 60 mol.%Pt, 40 mol.%IrO_2. Our future research will focus on identifying reasons for the higher stability of double-layer anodes as compared to titanium anodes coated with 60 mol.%Pt, 40 mol.%IrO_2. The compact second layer formed of iridium dioxide and metallic platinum most likely prevents the dissolution of RuO_2 and hence pore development. The interlayer made of the solid solution of ruthenium and titanium dioxides provides good adhesion of the coating to the titanium metal substrate. The good adhesion and lack of pores prevent the formation of poorly conductive titanium oxides in the titanium metal–coating interphase and, hence, anode passivation.

The results presented suggest that the titanium anode containing an active double-layer RuO_2, TiO_2, IrO_2, Pt coating can be used in the electrochemical production of chlorine, chlorate and active chlorine and some metals from their dilute acid sulfate solutions due to its high catalytic activity, good selectivity of electrochemical reactions and high corrosion stability.

4. Conclusion

A double-layer nanostructured electrochemically active coating was thermally deposited on a titanium metal substrate at 500 °C. The first layer of the coating was made from rutile-structured nanocrystals of a solid solution of ruthenium and titanium dioxides, 40 mol.%RuO_2, 60 mol.%TiO_2, with the average crystal grain size of 30 nm. The second layer consists of a mixture of amorphous particles of metallic platinum and

rutile-structured iridium dioxide nanocrystals having an average crystal grain size of 26 nm.

Nanocrystals of both rutile phases are characterized by a high density of chaotically distributed dislocations and high microstrains. The double-layer coatings exhibit a compact granular morphology. The coatings obtained at 500 °C develop no cracks on the surface. The catalytic activity of the anodes containing these active coatings is almost identical to that of DSAs for anodic oxidation of chloride ions from both concentrated and dilute sodium chloride solutions. The anodic current efficiency of both chlorate and active chlorine electrolyzers using double-layer electrodes is several percentage points higher than that in electrolyzers which use conventional DSAs.

The catalytic activity of the double-layer coating is about 50 mV lower than that of DSAs and about 350 mV higher than that of conventional lead/antimony alloy electrodes, for oxygen evolution from acid sulfate solutions. An accelerated corrosion test showed that the stability of the anodes with double-layer coatings is about twelve-fold higher than that of conventional DSAs.

Acknowledgment

The financial support from the Ministry of Education and Science of the Republic of Serbia Project No. 172 057 is acknovledged.

References

[1] S. Trasatti, G. Lodi, Electrodes of Conductive Metallic Oxides, Part B, Elsevier, Amsterdam, 1981.
[2] A. Nidola, Electrodes of Conductive Metallic Oxides, Part B, Elsevier, Amsterdam, 1981.
[3] K.L. Hordee, L.K. Mitchell, The influence of electrolyte parameters on the percent oxygen evolved from a chlorate cell, Journal of the Electrochemical Society 136 (1989) 3314–3318.
[4] N. Ibl, H. Vogt, Comprehensive Treatise of Electrochemistry, vol. 2, Plenum Press, New York, 1981.
[5] M. Spasojević, N. Krstajić, M. Jakšić, Optimization of an anodic electrocatalyst: RuO_2/TiO_2 on titanium, Journal of Research Institute for Catalysis Hokkaido Univiversity 31 (1983) 77–94.
[6] N. Krstajić, M. Spasojević, M. Jakšić, A selective catalyst for titanium anodes: development and optimization: I. Catalyst structure, activity and durability, Journal of Research Institute for Catalysis Hokkaido Univiversity 32 (1984) 19–28.
[7] M. Spasojević, N. Krstajić, M. Jakšić, A selective catalyst for titanium anodes: development and optimization: II. Selectivity features, Journal of Research Institute for Catalysis Hokkaido Univiversity 32 (1984) 29–36.
[8] N. Krstajić, M. Spasojević, M. Jakšić, A selective catalyst for titanium anodes, Journal of Molecular Catalysis 38 (1986) 81–84.
[9] M. Spasojević, N. Krstajić, M. Jakšić, Electrocatalytic optimization of faradaic yields in the chlorate cell process, Surface Technology 21 (1984) 19–24.
[10] N. Krstajić, V. Nakić, M. Spasojević, Hypochlorite production. I. A model of the cathodic reactions, Journal of Applied Electrochemistry 17 (1987) 77–81.
[11] P. Byrne, E. Fontes, G. Lindbergh, O. Parhammar, Chlor-Alkali and Chlorate Technology, The Electrochemical Society Proceedings Series, Pennington, 1999.
[12] J. Wanngard, Modern Chlor-Alkali Technology, vol. 5, Elsevier Appl. Sci., London and New York, 1992.
[13] L.M. Elina, V.M. Gitneva, V.I. Bystrov, N.M. Shmygul, Primenenie okisloruteniievuh anodov v hloratnom elektrolize, Elektrokhimiya 10 (1974) 68–70.
[14] V.I. Eberil, N.S. Fedotova, E.A. Novikov, Polarization characteristics of DSA anodes in the conditions of obtaining sodium chlorate, Elektrokhimiya 33 (1997) 563–569.
[15] V.I. Eberil, Yu.V. Doborov, E.A. Novikov, N.S. Fedotova, The current efficiency for chlorate and current losses due to oxygen formation as a function of anodic potential in the electrolysis of chloride–chlorate solutions at RTO anodes, Elektrokhimiya 33 (1997) 570–572.
[16] V.I. Eberil, N.S. Fedotova, E.A. Novikov, Polarization characteristics of metal-oxide anodes based on ruthenium, iridium, and titanium oxides: a comparison with traditional DSA in the conditions pertaining to sodium chlorate production, Elektrokhimiya 33 (1997) 660–663.
[17] V.I. Eberil, N.S. Fedotova, E.A. Novikov, A.F. Mazanko, Studying the link between the potential of a metal-oxide anode,the current efficiency for chlorate, and the current losses for the oxygen and chlorine evolution in a wide range of the chlorate electrolysis conditions, Elektrokhimiya 36 (2000) 1296–1302.
[18] S.W. Evdokimov, Electrochemical and corrosion behavior of dimensionally stable anodes in chlorate electrolysis: efficiency of the sodium chlorate production at elevated temperatures, Elektrokhimiya 37 (2001) 363–371.
[19] B.V. Tilak, C.P. Chen, Chlor-alkali and Chlorate Technology, The Electrochemical Society Proceedings Series, Pennington, NJ, PV, 1999.
[20] P. Byrne, E. Fontes, G. Lindbergh, O. Parhammar, A simulation of the tertiary current density distribution from a chlorate cell: I. Mathematical model, Journal of the Electrochemical Society 148 (2001) 125–132.
[21] A. Cornell, B. Hakansson, G. Lindbergh, Ruthenium based DSA® in chlorate electrolysis—critical anode potential and reaction kinetics, Electrochimica Acta 48 (2003) 473–481.
[22] T. Lassali, J. Boodts, S. Trassati, Electrocatalytic activity of the ternary oxide $Ru_{0.3}Pt_xTi_{(0.7-x)}O_2$ for chlorine evolution, Electrochimica Acta 39 (1994) 1545–1549.
[23] S. Barison, A.D. Battisti, M. Fabrizio, S. Daollo, C. Piccirillo, Surface chemistry of $RuO_2/IrO_2/TiO_2$ mixed-oxide electrodes: secondary ion mass spectrometric study of the changes induced by electrochemical treatment, Rapid Communications in Mass Spectrometry 14 (2000) 2165–2169.
[24] S. Ferro, A. De Battisti, I. Duo, C. Comninellis, W. Haenni, A. Perret, Chlorine evolution at highly boron-doped diamond electrodes, Journal of the Electrochemical Society 147 (2000) 2614–2619.
[25] H.J. Jeong, H.R. Kim, K.I. Kim, K.Y. Kim, NaOCI produced by electrolysis of natural seawater as a potential method to control marine red-tide dinoflagellates, Phycologia 41 (2002) 643.
[26] S. Barison, S. Daolio, M. Fabrizio, A.D. Battisti, Surface chemistry study of $RuO_2/IrO_2/TiO_2$ mixed-oxide electrodes, Rapid Communications in Mass Spectrometry 18 (2004) 278–284.
[27] G. Spagnoletto, Innovation in food grade hypochlorination generation and injection plant at Al Taweelah site, Desalination 182 (2005) 259–265.
[28] X.M. Chen, G.H. Chen, Stable $Ti/RuO_2–Sb_2O_5–SnO_2$ electrodes for O_2 evolution, Electrochimica Acta 50 (2005) 4155–4159.
[29] D. Rajkumar, J.G. Kim, Oxidation of various reactive dyes with in situ electro-generated active chlorine for textile dyeing industry wastewater treatment, Journal of Hazardous Materials 136 (2006) 203–212.
[30] Y. Kiros, M. Pirjamali, M. Bursell, Oxygen reduction electrodes for electrolysis in chlor-alkali cells, Electrochimica Acta 51 (2006) 3346–3350.
[31] Z. Yi, C. Kangning, W. Wei, J. Wang, S. Lee, Effect of IrO_2 loading on $RuO_2–IrO_2–TiO_2$ anodes: a study of microstructure and working life for the chlorine evolution reaction, Ceramics International 33 (2007) 1087–1091.
[32] V.V. Panić, V.M. Jovanović, S.I. Terzić, M.W. Barsoum, V.D. Jović, A.B. Dekanski, The properties of electroactive ruthenium oxide coatings supported by titanium-based ternary carbides, Surface and Coatings Technology 202 (2007) 319–324.
[33] R. Thangappan, S.T. Sampathkumaran, Electrochlorination system: a unique method of prevention of biofouling in seawater desalination, International Journal of Nuclear Desalination 3 (2008) 135–142.

[34] A. Khelifa, S. Aoudj, S. Moulay, M. Hecini, M. De Petris-Werr, Degradation of EDTA by in situ electrogenerated active chlorine in electroflotation cell, Desalination and Water Treatment Science and Engineering 7 (2009) 119–123.
[35] D. Ghernaout, B. Ghernaout, From chemical disinfection to electrodisinfection: the obligatory itinerary? Desalination and Water Treatment Science and Engineering 16 (2010) 156–175.
[36] L. Petkov, Electrooxidation of chloride systems, Oxidation Communications 32 (2009) 654–678.
[37] H.A. Hansen, I.C. Man, F. Studt, F. Abild-Pedersen, T. Bligaard, J. Rossmeisl, Electrochemical chlorine evolution at rutile oxide (1 1 0) surfaces, Physical Chemistry Chemical Physics 12 (2010) 283–290.
[38] S. Chen, Y. Zheng, S. Wang, X. Chen, Ti/RuO_2–Sb_2O_5–SnO_2 electrodes for chlorine evolution from seawater, Chemical Engineering Journal 172 (2011) 47–51.
[39] S. Trasatti, Interfacial Electrochemistry: Theory, Experiment and Applications, Marcel Dekker, New York, 1999.
[40] F. Hine, M. Yasuda, T. Noda, T. Yoshida, J. Okuda, Electrochemical behavior of the oxide-coated metal anodes, Journal of the Electrochemical Society 126 (1979) 1439–1445.
[41] G. Lodi, E. Sivieri, A. de Battisti, S. Trassati, Ruthenium dioxide-based film electrodes, Journal of Applied Electrochemistry 8 (1978) 135–143.
[42] Y.E. Roginskaya, T.V. Varlamova, M.D. Goldstein, I.D. Belova, B.S. Galimov, R.R. Shifrina, V.A. Shepelin, Formation, structure and electrochemical properties of IrO_2–RuO_2 oxide electrodes, Materials Chemistry and Physics 30 (1991) 101–113.
[43] R. Hutchings, K. Muller, K.S. Stucki, A structural investigation of stabilized oxygen evolution catalysts, Journal of Materials Science 19 (1984) 3984–3987.
[44] R.T. Atanasoski, B.Ž. Nikolić, M.M. Jakšić, A.R. Despić, Platinum–iridium catalyzed titanium anode. I. Properties and use in chlorate electrolysis, Journal of Applied Electrochemistry 5 (1975) 155–158.
[45] R.T. Atanasoski, B.Ž. Nikolić, M.M. Jakšić, A.R. Despić, Platinum–iridium catalyzed titanium anode. II. Oxygen evolution, Journal of Applied Electrochemistry 5 (1975) 159–163.
[46] A.T. Kuhn, C.J. Mortimer, The efficiency of chlorine evolution in dilute brines on ruthenium dioxide electrodes, Journal of Applied Electrochemistry 2 (1972) 283–287.
[47] P.C.S. Hayfield, W.R. Jacob, Platinum/iridium-coated titanium anodes in brine electrolysis, in: M.O. Coulter (Ed.), Modern Chlor-alkali Technology, Ellis Horwood Ltd., Chichester, 1980 (Chapter 9).
[48] E.N. Balko, P.H. Nguyen, Iridium–tin mixed oxide anode coatings, Journal of Applied Electrochemistry 21 (1991) 678–682.
[49] L.A. Da Silva, V.A. Alves, M.A.P. da Silva, S. Trasatti, J.F.C. Boodts, Oxygen evolution in acid solution on IrO_2 + TiO_2 ceramic films. A study by impedance, voltammetry and SEM, Electrochimica Acta 42 (1997) 271–281.
[50] A. Benedetti, P. Riello, G. Battaglin, A. De Battisti, A. Barbieri, Physicochemical properties of thermally prepared Ti-supported IrO_2 + ZrO_2 electrocatalysts, Journal of Electroanalytical Chemistry 376 (1994) 195–202.
[51] H. Tamura, C. Iwakura, Metal oxide anodes for oxygen evolution, International Journal of Hydrogen Energy 7 (1982) 857–865.
[52] G. Chen, X. Chen, P.L. Yue, Electrochemical behavior of novel Ti/IrO_x–Sb_2O_5–SnO_2 anodes, Journal of Physical Chemistry B 106 (2002) 4364–4369.
[53] W. Yao, J. Yang, J. Wang, Y. Nuli, Chemical deposition of platinum nanoparticles on iridium oxide for oxygen electrode of unitized regenerative fuel cell, Electrochemistry Communications 9 (2007) 1029–1034.
[54] H.M. Villas, F.I. Mattos-Costa, P.A.P. Nascente, L.O.S. Bulhões, Structural and magnetic properties of a new type of ordered oxygen-deficient perovskite, $KMnVO_4$, Chemistry of Materials 19 (2007) 5563–5569.
[55] L.A. Da Silva, V.A. Alves, S. Trasatti, J.F.C. Bovdts, Surface and electrocatalytic properties of ternary oxides $Ir_{0.3}Ti_{(0.7-x)}Pt_xO_2$. Oxygen evolution from acidic solution, Journal of Electroanalytical Chemistry 427 (1997) 97–104.
[56] R. Kötz, S. Stucki, Stabilization of RuO_2 by IrO_2 for anodic oxygen evolution in acid media, Electrochimica Acta 31 (1986) 1311–1316.
[57] Y. Kamegaya, K. Sasaki, M. Oguri, T. Asaki, H. Hohayaski, T. Mitamura, Improved durability of iridium oxide coated titanium anode with interlayers for oxygen evolution at high current densities, Electrochimica Acta 40 (1995) 889–895.
[58] S. Trasatti, The Electrochemistry of Novel Materials, VCH, Weinheim, 1994.
[59] G.P. Vercesi, J.Y. Salamin, Ch. Comninellis, Morphological and microstructural the Ti/IrO_2 Ta_2O_5 electrode: effect of the preparation temperature, Electrochimica Acta 36 (1991) 991–998.
[60] J. Rolewicz, Ch. Comninellis, E. Plattner, J. Hinden, Charactérisation des électrodes de type DSA pour le dégagement de O_2—I. L'électrode Ti/IrO_2 Ta_2O_5, Electrochimica Acta 33 (1988) 573–580.
[61] Ch. Comninellis, G.P. Vercesi, Problems in DSA® coating deposition by thermal decomposition, Journal of Applied Electrochemistry 21 (1991) 136–142.
[62] Ch. Comninellis, G.P. Cercesi, Characterization of DSA®-type oxygen evolving electrodes: choice of a coating, Journal of Applied Electrochemistry 21 (1991) 335–345.
[63] M. Spasojević, L. Ribić-Zelenović, A. Maričić, The phase structure and morphology of electrodeposited nickel-cobalt alloy powders, Science of Sintering 43 (2011) 313–326.
[64] E.A. Kalonovskii, R.U. Bondar, N.N. Meshkova, Nerastvorimui titandvuokisnorutenievui anod dlya elektroliza hloridov, Elektrokhimiya 8 (1972) 1468–1471.
[65] V.I. Bystrov, O.P. Romashin, Polyarizatsionnue izmereniya s okisnorutenievumi anodami razlichnogo sostava, Elektrokhimiya 11 (1975) 1226–1227.
[66] T. Loucka, The reason for the loss of activity of titanium anodes coated with a layer of RuO_2 and TiO_2, Journal of Applied Electrochemistry 7 (1977) 211–214.
[67] V.I. Bystrov, O prichinah vozrastaniya potenciala metallookisnuh anodov s titanovoi osnovoi, Elektrokhimiya 11 (1975) 1902.
[68] S. Ardizzone, G. Fregonara, S. Trasatti, Inner and outer active surface of RuO_2 electrodes, Electrochimica Acta 35 (1990) 263–267.
[69] F. Ye, J. Li, X. Wang, T. Wang, S. Li, E. Christensen, Electrocatalytic properties of Ti/Pt–IrO_2 anode for oxygen evolution in PEM water electrolysis, International Journal of Hydrogen Energy 35 (2010) 8049–8055.